Supporting materials

Rapid Construction of Co/CoO/CoCH Nanowire Core/Shell Arrays for Highly Efficient Hydrogen Evolution Reaction

Sihan Liu, [a] Runwei Song, [a, b] Shuai Wang, [a] Weiye Shi, [a] Qin Zhou, [a] Yan Zhang, [a] Chunqing Huo, *[a] Shengjue Deng, *[a] and Shiwei Lin*[a]

a. School of Materials Science and Engineering, and State Key Laboratory of Marine Resource Utilization in South China Sea, Hainan University, Haikou 570228, P. R. China

b. CNOOC (Hainan) new energy Co. Ltd, Haikou, 570311, P. R. China

*Corresponding author. chunqinghuo@hainanu.edu.cn; 184305@hainanu.edu.cn; linsw@hainanu.edu.cn

Experimental details

CoCH electrodes were prepared on nickel foam (NF) substrate by hydrothermal method. Firstly, the NF was soaked in 3 M HCl for 5 min to remove the contaminants, and then the NF was sonicated in anhydrous ethanol and deionized water for 5 min respectively. The 0.87 g of $Co(NO_3)_2 \cdot 6H_2O$, 0.3 g of CH_4N_2O, and 0.1 g of NH_4F were dissolved in 30 ml of deionized water, and then the solution was transferred to a reaction kettle with a piece of NF. The reactor was kept at 120 ℃ for 6 h, and the sample was taken out and vacuum-dried at 60 ℃ for 2 h to obtain CoCH@NF. Then, the sample (CoCH@NF) was put into the quartz tube of plasma enhanced chemical vapor deposition (PECVD) and the P-CoCH@NF was obtained by treating CoCH@NF for 10 min under the mixed atmosphere of 10 sccm Ar/H_2. During the plasma treatment process, the RF power supply of PECVD was maintained at 400 W. For comparison, the C/Pt (20 % wt.) electrode (1 cm^2) with the same loading as P-CoCH@NF was prepared.

The surface morphology and element distribution of the samples were observed by scanning electron microscopy (SEM, JSM-7800F, JEOL). Transmission electron microscopy (TEM, JSM-2800, JEOL) was utilized to determine the structure of a sample through the lattice fringes. X-ray diffraction (XRD, Empyrean, Panalytical) was used to characterize the phase structure of the sample, and the test angle was 20-80°. X-ray photoelectron spectroscopy (XPS, Axis Supra) was used to analyze the surface elements and their chemical valence states. The binding energy of the test was corrected with C 1s (284.8 eV) as the standard.

All electrochemical performance tests were carried out in 1 M KOH solution by using an electrochemical workstation (Zahner Zennium) in a standard three-electrode system. CoCH@NF, P-CoCH@NF and C/Pt (20 % wt.) was used directly as the working electrode, and the working surface area was about 1 cm^2. A Hg/HgO electrode and a platinum electrode were used as the reference electrode and counter electrode, respectively. All tests were carried out at room temperature and atmospheric pressure. Electrochemical tests were carried out for cyclic voltammetry curve (CV), and linear scan voltammogram (LSV). The scan rate was 5 mV/s. The HER performance was analyzed through the obtained LSV and Tafel curve. All of the measured potential values were calibrated by using equation: $E_{RHE} = E_{Hg/HgO} + 0.098 + 0.059 \times pH$. Considering the internal resistance of the system, all LSV data was subjected to 95% current truncation compensation (IR compensation). The Tafel slope was calculated from the LSV curve after IR compensation. The electrochemically active surface area (ESCA) could be estimated from the double-layer capacitance value (C_{dl}), which was linearly fitted from the cyclic voltammetry (CV) in the non-Faradaic region. The selected potential scanning range was 0.424 ~ 0.524 V vs. RHE, and the scanning speed was 100, 80, 60, 40 and 20 mV/s, respectively. When the potential was the median value of the test range (0.474 V vs. RHE), the absolute value of the difference between the anode and cathode current density was linear with the scanning rate, and the value of $2 \times C_{dl}$ was equal to the slope of the fitted line. The value of C_{dl} has a linear relationship with ESCA. The higher the value of C_{dl}, the higher the chemically active surface area, which promotes the electrocatalytic water splitting process. The potential of the

electrochemical impedance test was -1.1 V vs. RHE, the frequency range of the test was 0.1 Hz ~100 kHz, and the amplitude was 10 mV. The stability test performed at 100 mA/cm^2 current density for 24 hours.

Fig. S1 The picture of NF, CoCH@NF, P-CoCH@NF samples.

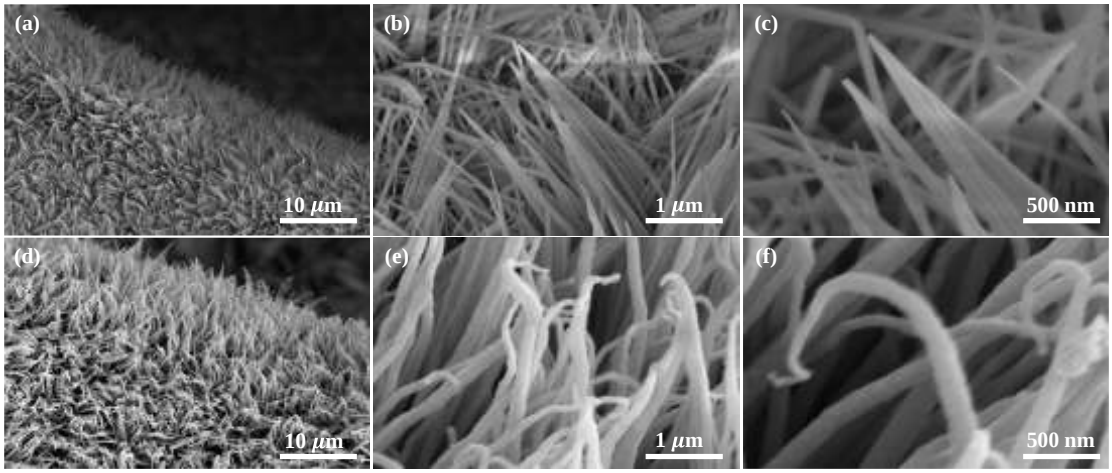

Fig. S2 (a-c) SEM images of CoCH@NF; (d-f) SEM images of P-CoCH@NF.

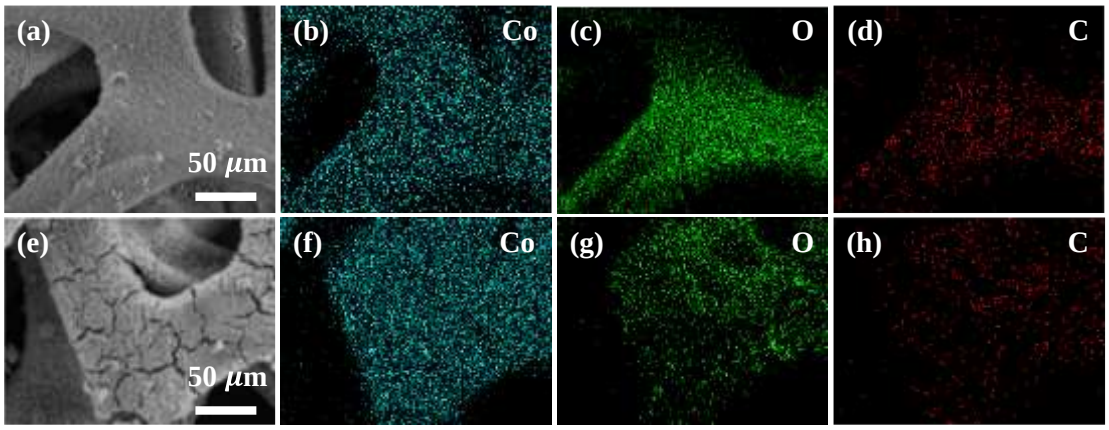

Fig. S3 (a) SEM image of CoCH@NF and corresponding EDS mapping images of (b) Co, (c) O and (d) C elements. (e) SEM image of P-CoCH@NF and corresponding EDS mapping images of (f) Co, (g) O and (h) C elements.

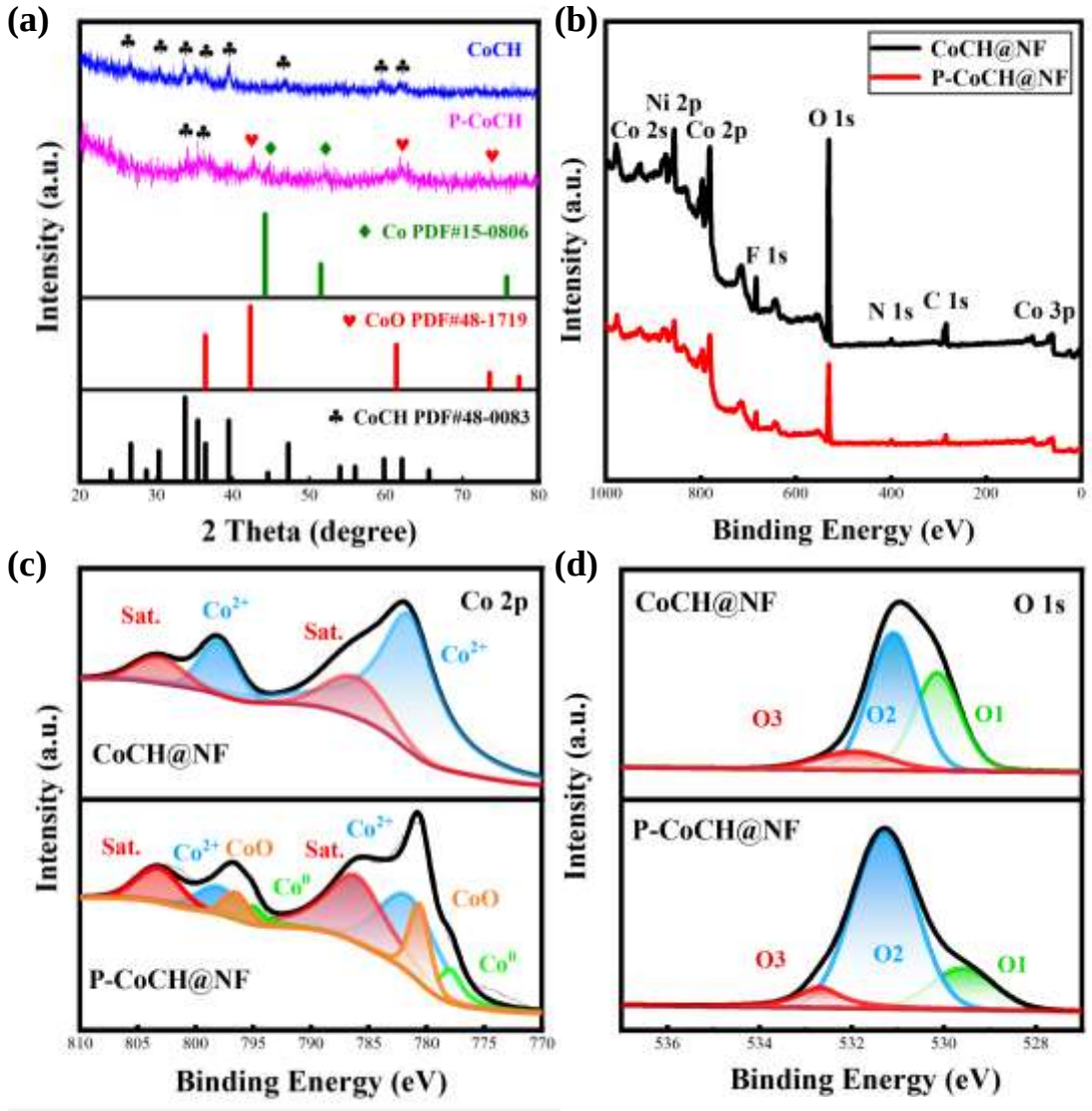

Fig. S4 (a) XRD patterns of CoCH and P-CoCH; (b) XPS full spectra of CoCH and P-CoCH; (c) Co 2p spectrum; (d) O 1s spectrum.

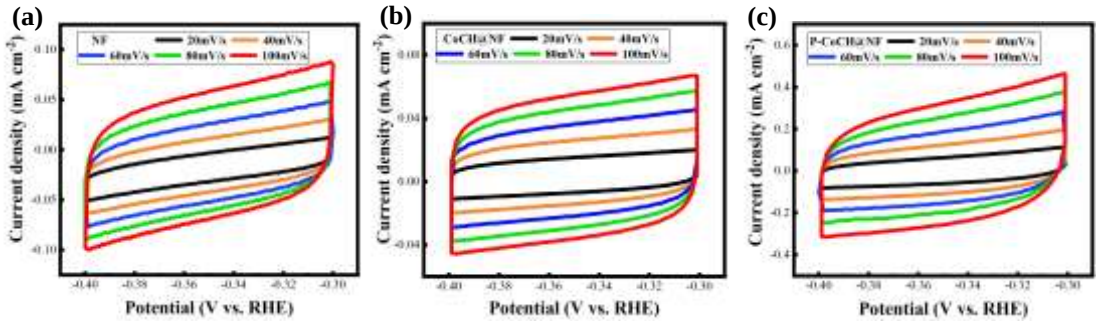

Fig. S5 CV curves at different scan rates from 20 to 100 mV/s of (a) NF, (b) CoCH@NF and (c) P-CoCH.

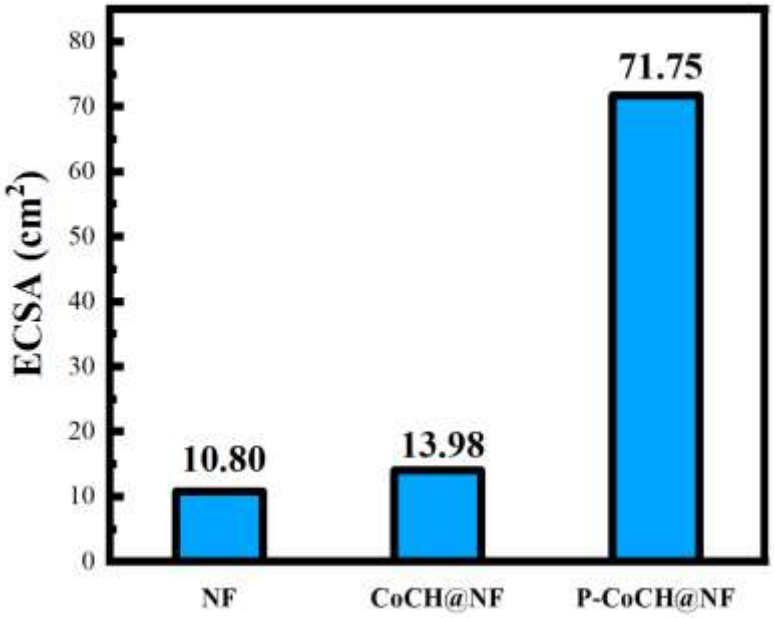

Fig. S6 The ECSA of NF, CoCH@NF and P-CoCH@NF.

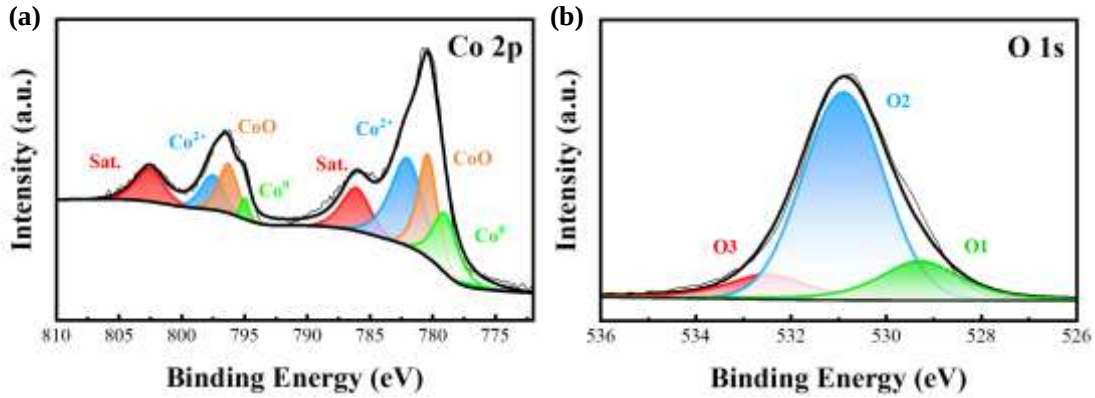

Fig. S7 XPS results of P-CoCH@NF after 24 h stability test, (a) Co 2p spectrum; (b) O 1s spectrum.

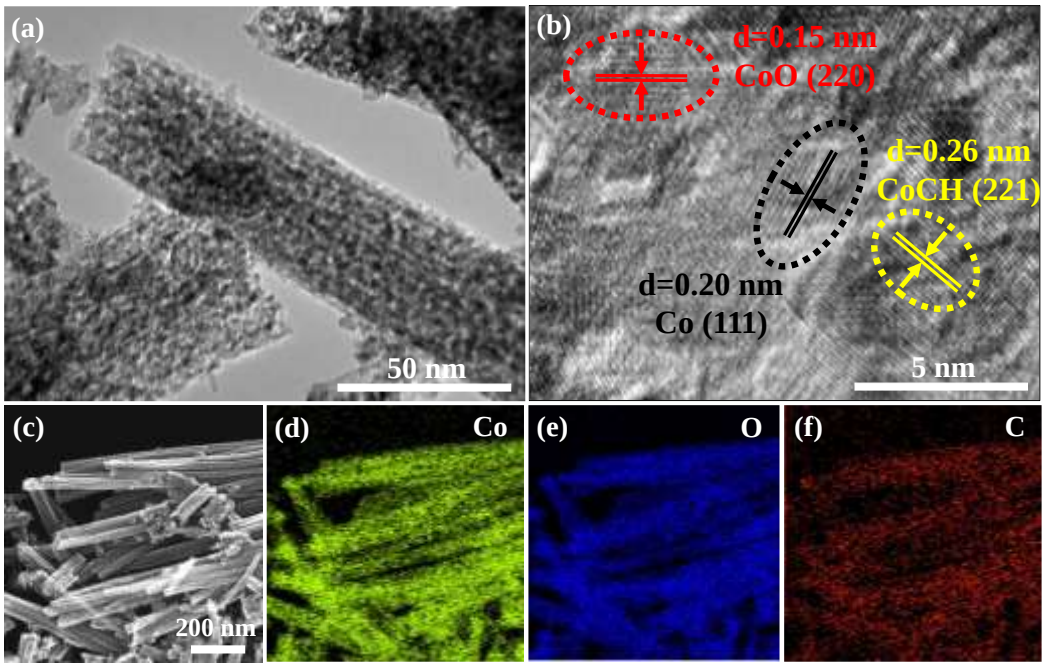

Fig. S8 (a) TEM and (b) HRTEM images of P-CoCH@NF after 24 h stability test; (c) HAADF-STEM image of P-CoCH@NF after 24 h stability test and corresponding EDS mapping images of (d) Co, (e) O and (f) C elements.

The XPS results of P-CoCH@NF after stability test are shown in Fig. S7, and the chemical valence state of Co and O elements did not change significantly. The sample after the stability test still maintained the structure of the nanowire core/shell arrays, as shown in Fig. S8. The distribution of Co, O and C elements also did not change significantly.

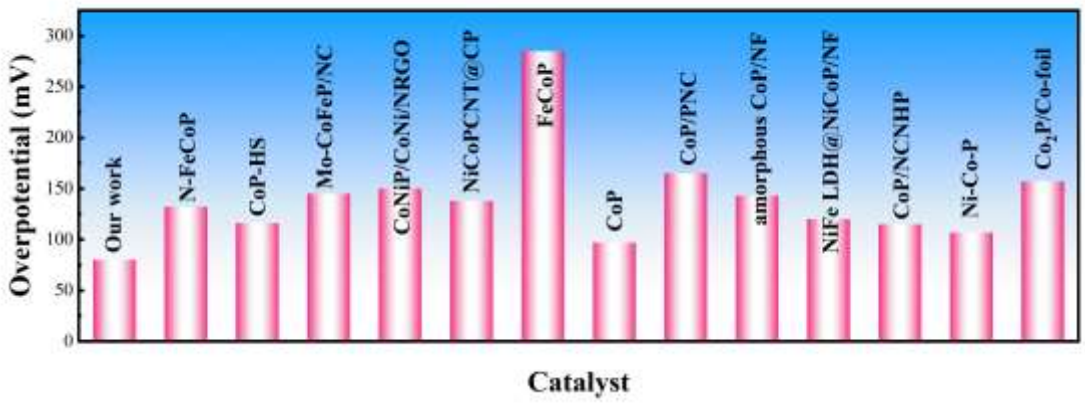

Fig. S9 Performances for HER of some recently reported materials. (Specific values are listed in Table S2.)

Table S1. Compositions of C, H and Co elements in the catalysts before and after the plasma treatment

Sample	C (%)	H (%)	Co (%)
CoCH@NF	3.968	1.632	36.903
P-CoCH@NF	1.170	0.870	41.929

Table S2. Comparison of HER performances of recently reported cobalt-based compounds electrocatalysts in alkaline media

Sample	Electrolyte (KOH)	HER E_{j10} (mV)	Tafel slope (mV/dec)	Refs
P-CoCH@NF	**1.0 M**	**69.0**	**47.0**	**This work**
N-FeCoP	1.0 M	132.0	79.0	[1]
CoP-HS	1.0 M	116.0	89.0	[2]
Mo-CoFeP/NC	1.0 M	145.0	68.0	[3]
CoNiP/CoNi/N-RGO	1.0 M	150.0	97.0	[4]
NiCoP-CNT@CP	1.0 M	138.0	145.0	[5]
FeCoP	1.0 M	285.0	153.0	[6]
CoP-MB	1.0 M	97.3	84.0	[7]
CoP/PNC	1.0 M	165.0	70.0	[8]
amorphous CoP/NF	1.0 M	143.0	63.0	[9]
NiFe LDH@NiCoP/NF	1.0 M	120.0	88.0	[10]
CoP/NCNHP	1.0 M	115.0	66.0	[11]
Ni–Co–P HNB	1.0 M	107.0	46.0	[12]
Co_2P/Co-foil	1.0 M	157.0	59.0	[13]

Reference:

[1] Z. Liu, T. Zhang, Y. Lin, H. Jia, Y. Wang, Y. Wang, G. Zhang, Highly N-Doped Fe/Co Phosphide Superstructures for Efficient Water Splitting, Small 2023 n/a E2302475.

[2] W. Zhang, N. Han, J. Luo, X. Han, S. Feng, W. Guo, S. Xie, Z. Zhou, P. Subramanian, K. Wan, J. Arbiol, C. Zhang, S. Liu, M. Xu, X. Zhang, J. Fransaer, Critical Role of Phosphorus in Hollow Structures Cobalt-Based Phosphides as Bifunctional Catalysts for Water Splitting, Small 2022 18 2103561.

[3] R. Fu, X. Jiao, J. Yu, Q. Jiao, C. Feng, Y. Zhao, Mo-Doped CoFeP/Nitrogen Doped Carbon Porous Nanocubes for Alkaline Hydrogen Production, J. Electroanal. Chem. 2023 930 117137.

[4] P. Arunkumar, S. Gayathri, J.H. Han, A Complementary Co−Ni Phosphide/Bimetallic Alloy-Interspersed N-Doped Graphene Electrocatalyst for Overall Alkaline Water Splitting, Chemsuschem 2021 14 1921-1935.

[5] Z. Wang, C. Wei, X. Zhu, X. Wang, J. He, Y. Zhao, A Hierarchical Carbon Nanotube Forest Supported Metal Phosphide Electrode for Efficient Overall Water Splitting, J. Mater. Chem. A 2021 9 1150-1158.

[6] Y. Wen, S. Xu, P. Wang, X. Shao, X. Sun, J. Hu, X.-R. Shi, Bimetallic FeCo Phosphide Nanoparticles Anchored on N-Doped Carbon Foam for Wide pH Hydrogen Evolution Reaction, J. Alloys Compd. 2023 931 167570.

[7] H. Cao, Y. Xie, H. Wang, F. Xiao, A. Wu, L. Li, Z. Xu, N. Xiong, K. Pan, Flower-Like CoP Microballs Assembled with (002) Facet Nanowires via Precursor Route: Efficient Electrocatalysts for Hydrogen and Oxygen Evolution, Electrochim. Acta 2018 259 830-840.

[8] Z. Peng, Y. Yu, D. Jiang, Y. Wu, B.Y. Xia, Z. Dong, N-Doped Carbon Shell Coated CoP Nanocrystals Encapsulated in Porous N-Doped Carbon Substrate as Efficient Electrocatalyst of Water Splitting, Carbon 2019 144 464-471.

[9] R. Beltrán-Suito, P.W. Menezes, M. Driess, Amorphous Outperforms Crystalline Nanomaterials: Surface Modifications of Molecularly Derived CoP Electro(pre)catalysts for Efficient Water-Splitting, J. Mater. Chem. A 2019 7 15749-15756.

[10] H. Zhang, X. Li, A. Hähnel, V. Naumann, C. Lin, S. Azimi, S.L. Schweizer, A.W. Maijenburg, R.B. Wehrspohn, Bifunctional Heterostructure Assembly of NiFe LDH Nanosheets on NiCoP Nanowires for Highly Efficient and Stable Overall Water Splitting, Adv. Funct. Mater. 2018 28 1706847.

[11] Y. Pan, K. Sun, S. Liu, X. Cao, K. Wu, W.C. Cheong, Z. Chen, Y. Wang, Y. Li, Y. Liu, D. Wang, Q. Peng, C. Chen, Y. Li, Core-Shell Zif-8@Zif-67-Derived CoP Nanoparticle-Embedded N-Doped Carbon Nanotube Hollow Polyhedron for Efficient Overall Water Splitting, J. Am. Chem. Soc. 2018 140 2610-2618.

[12] E. Hu, Y. Feng, J. Nai, D. Zhao, Y. Hu, X.W. Lou, Construction of Hierarchical Ni–Co–P Hollow Nanobricks with Oriented Nanosheets for Efficient Overall Water Splitting, Energy Environ. Sci. 2018 11 872-880.

[13] C.Z. Yuan, S.L. Zhong, Y.F. Jiang, Z.K. Yang, Z.W. Zhao, S.J. Zhao, N. Jiang, A.W. Xu, Direct Growth of Cobalt-Rich Cobalt Phosphide Catalysts on Cobalt Foil: An Efficient and Self-Supported Bifunctional Electrode for Overall Water Splitting in Alkaline Media, J. Mater. Chem. A 2017 5 10561-10566.